RESEARCH ARTICLE

ADVANCED MATERIALS INTERFACES Open Access

www.advmatinterfaces.de

Using a Zero-Strain Reference Electrode to Distinguish Anode and Cathode Volume Changes in a Solid-State Battery

*Mervyn Soans, Benedikt Huber, Marcel Drüschler, Dominic Bresser, Alberto Varzi, and Christoffer Karlsson**

Solid-state battery electrodes expand and contract during cycling ("cell breathing"), which can cause cracking of the active material particles. This lowers their electronic conductivity, leading to inactive regions, and is the main cause of capacity fading for many electrode chemistries, including nickel-rich $LiNi_{1-x-y}Mn_xCo_yO_2$ (NMC). The active material volume change because of (de)lithiation is known as the reaction volume and can be calculated from the change in open-circuit potential when varying the applied pressure. In order to determine the reaction volume in this way for both anode and cathode simultaneously, a "zero-strain" reference electrode (i.e., without volume changes) must be used, as its potential remains constant with varying pressure. Herein, the study uses a reference electrode based on $Li_4Ti_5O_{12}/Li_7Ti_5O_{12}$ to measure the reaction volume for both electrodes in solid-state battery cells. For a graphite||NMC cell, the total pressure change measured during cycling can be separated into the individual contributions of graphite and NMC. Graphite is responsible for most of the cell breathing, except at the end of charge, where the NMC contraction counteracted the graphite expansion, leading to a pressure plateau. This method reveals detailed information about the breathing of the individual electrodes without the need for complementary characterization techniques.

1. Introduction

Solid-state batteries are emerging as an alternative to conventional liquid-electrolyte batteries, but are not immune to the volume changes associated with cell failure and capacity fading that are present in both those types of cells.[1–3] In fact, the impact on performance is more severe for solid-state cells.[1,4] Lithium-ion battery electrodes expand and contract during charge and discharge, in some cases leading to cracking of the active material particles, reducing electronic contact and increasing electrode impedance.[4,5] Eventually, the available cell capacity decreases as the whole electrode material can no longer be utilized. Electrode volume changes have been identified as the main root cause for capacity fading of nickel-rich $LiNi_{1-x-y}Mn_xCo_yO_2$ (NMC) cathodes[4,5] as well as silicon anodes.[6,7] Therefore, it is imperative to quantify the volume changes of the active materials employed in solid-state batteries in order to improve their cyclability.

The origin of the active material volume changes is the uptake/release of lithium ions into/from their chemical structure. The difference in molar volume (V_m) of the structure before and after the (de)lithiation reaction is expressed by the (molar) reaction volume ($\Delta_r V_m$).[8] For example, the reaction volume of the lithiation of indium corresponds to the difference in molar volume between In and InLi, while the reaction volume of lithium is identical to its molar volume.[8] The reaction volume can be calculated from the molar volumes based on crystallographic data, but this approach is not convenient for insertion and intercalation materials, which make up most of the solid-state battery electrodes, since the reaction volume is not constant for a varying state of charge (SOC).[8–11] For such materials, the reaction volume is the same as the partial molar volume of lithium, *i.e.*, the change in volume for a certain change in lithium content.[8] The reaction volume can also be calculated by examining the dependence of the open-circuit potential (OCP) on the applied pressure, as described in the Experimental Section. However, this is complicated by the fact that the individual electrode potentials are unknown in a two-electrode cell, as only the overall cell voltage can be measured. The use of an

M. Soans, D. Bresser, A. Varzi
Helmholtz Institute Ulm (HIU)
89081 Ulm, Germany
M. Soans, D. Bresser, A. Varzi
Karlsruhe Institute of Technology (KIT)
76021 Karlsruhe, Germany
B. Huber, M. Drüschler, C. Karlsson
rhd instruments GmbH & Co. KG
64293 Darmstadt, Germany
E-mail: karlsson@rhd-instruments.de
D. Bresser
Ulm University (Ulm)
89069 Ulm, Germany

The ORCID identification number(s) for the author(s) of this article can be found under https://doi.org/10.1002/admi.202500709

DOI: 10.1002/admi.202500709

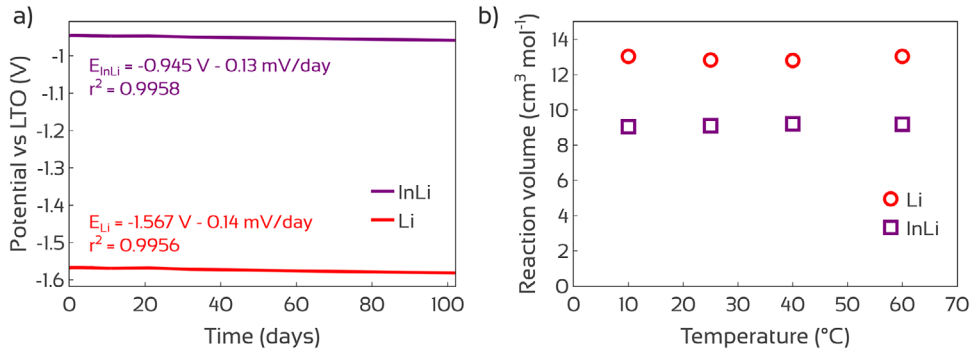

Figure 1. a) Stability of the LTO reference electrode: Potential of InLi (purple) and Li (red) versus LTO for 100 days (25 °C, 5 MPa). The inset text describes linear fits of the potential behavior over time. b) Reaction volume of Li (red circles) and InLi (purple squares) versus temperature.

$Li_4Ti_5O_{12}/Li_7Ti_5O_{12}$ (LTO) counter electrode solves this problem, since LTO is a so-called "zero-strain" material, with close to zero reaction volume.[12] Hence, the measured reaction volume of a cell with an LTO counter electrode can be attributed exclusively to the other (working) electrode.[8] Nevertheless, this precludes the possibility of measuring the reaction volume in situ in a full cell with both the anode and cathode being of interest. A three-electrode solid-state cell where the potentials of both electrodes can be measured separately and simultaneously with respect to a known pressure-independent reference potential would be required to enable such a measurement. To our knowledge, simultaneous determination of the reaction volumes of both electrodes has so far not been reported. One complicating issue is that the reference electrode potential is typically also affected by the applied pressure, which needs to be addressed in order to accurately assign the reaction volume to each electrode.

In this study, we describe a three-electrode solid-state setup with a zero-strain reference electrode based on LTO. Using this reference electrode with a pressure-independent potential, the reaction volumes of both electrodes were simultaneously measured in solid-state battery cells in situ. The pressure changes during cycling of a graphite||NMC cell could be separated into the contribution from graphite and NMC, revealing important insights for the design and operation of such cells – especially when transitioning to large-format cells.

2. Results and Discussion

2.1. LTO Reference Electrode Evaluation

Reference electrodes based on LTO have only rarely been employed in solid-state battery research so far.[13,14] When employed as a reference electrode in a Li|LPSCl|InLi cell, LTO has a potential of 1.57 V versus Li and 0.94 V versus InLi (at 25 °C, 20 MPa). Since this is much less reducing in nature than either Li or InLi, it might be more compatible with a wide range of solid electrolytes, that would otherwise experience unwanted side-reactions with a Li or InLi reference electrode. For example, Li-metal-based reference electrodes are typically only stable for a few days since Li is far outside the thermodynamic stability window of sulfidic electrolytes.[15–17] The LTO reference electrode exhibited a stable potential for at least 100 days in the Li|LPSCl|InLi cell, with a drift of less than 0.2 mV per day (**Figure 1a**). However, repeated pressure application and release lead to faster potential drift, likely due to mechanical shearing of the LTO coating and detachment from the current collector wire. The mechanical stability of the reference electrode could be improved by optimizing the coating procedure.

The primary advantage of LTO as a reference electrode material is that its reduction potential is invariable with pressure, arising from the fact that the reaction volume of LTO is close to zero, i.e., the oxidized and reduced structures ($Li_4Ti_5O_{12}$ and $Li_7Ti_5O_{12}$, respectively) have the same molar volume (within 0.2%).[12] Other reference electrode materials, such as Li metal exhibit a varying reduction potential depending on the applied pressure, meaning that measurements performed at different pressures cannot be easily compared. LTO, on the other hand, serves as a fixed reference point for potential measurements in solid-state cells. Increasing the applied pressure in the Li|LPSCl|InLi cell reveals linearly decreasing potentials of Li and InLi versus LTO (Figures S1–S3, Supporting Information), allowing for the extrapolation of the reduction potential to zero pressure for Li (-1.565 V vs LTO) and InLi (-0.943 V vs LTO). These pressure-independent reduction potentials can be used when measuring potentials versus Li or InLi, (see Equation (3) in the Experimental Section).

2.2. Reaction Volume of Li and InLi

The reaction volumes of Li and InLi at different temperatures can be calculated from the respective slopes of the potential versus pressure (Figure 1b; Figures S2 and S3, Supporting Information). At 25 °C, a reaction volume of 12.8 and 9.1 $cm^3\ mol^{-1}$ was measured for Li and InLi, respectively. The reaction volume between 10 and 60 °C was constant for both Li and InLi, which is expected since the molar volumes of Li (13 $cm^3\ mol^{-1}$), In (16 $cm^3\ mol^{-1}$), and InLi (24 $cm^3\ mol^{-1}$) all change less than 1% in this temperature range.[18–20] The measured values are in good agreement with those expected by crystallographic data, supporting that the LTO reference potential is, in fact, pressure-independent in this cell configuration. The small deviations of the experimentally determined reaction volume might arise from non-ideal crystal structures formed during electrochemical lithiation.[3] This is much more severe for a Li metal reference electrode,[15] since it is composed of a microscopic amount of Li metal with a

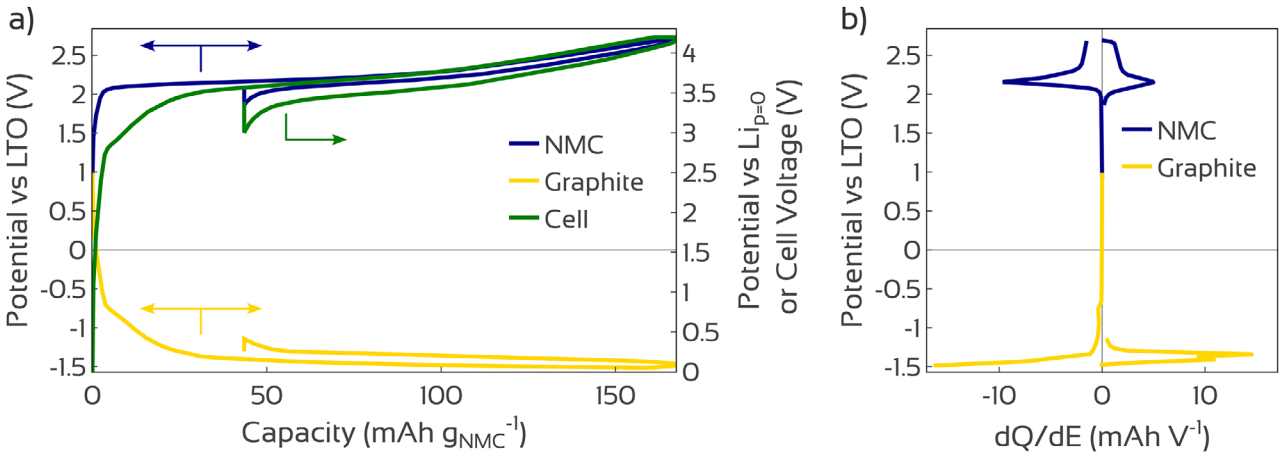

Figure 2. First cycle of a three-electrode graphite|LPSCl|NMC cell with an LTO reference electrode. a) Individual NMC cathode (blue) and graphite anode (yellow) potentials versus LTO (left y-axis) and versus Li (zero-pressure, right y-axis), as well as cell voltage (green, right y-axis). b) Differential capacity (dQ/dE) distribution for graphite (yellow) and NMC (blue). The charging process is shown as negative dQ/dE while the discharge is positive.

significant amount of disorder and a relatively small amount of crystalline bulk lithium.[21] This makes the reaction volume determination in a three-electrode setup very challenging when using most reference electrode materials, as the contribution from the pressure/potential dependence of the reference electrode itself cannot be easily excluded. For this reason, the use of a zero-strain reference electrode such as LTO is crucial for the accurate and simultaneous measurement of both anode and cathode reaction volumes in situ.

2.3. Graphite||NMC Full Cell Cycling

A reference electrode allows for differentiating the anode and cathode contributions to the cell voltage, as shown for the first cycle of a graphite|LPSCl|NMC cell in **Figure 2**. This facilitates the assignment of certain cell voltage features to either electrode.[15] For example, the initial sloping feature at 2.8–3.5 V cell voltage during the first charge can be assigned to the graphite anode. The distributions of potentials where each electrode exhibits capacity can be seen in the differential capacity plot in Figure 2b, and in more detail in Figure S6 (Supporting Information). The graphite anode showed an increasing dQ/dE until the end of the charge step (-1.52 V vs LTO), while the discharge displayed two separate dQ/dE peaks at -1.41 and -1.34 V versus LTO, corresponding to lithium deintercalation stage I and II, respectively.[11,22] The NMC cathode exhibited its main redox peak at 2.16 V versus LTO, as well as some additional capacity above 2.3 V versus LTO. A large portion (26%) of the initial charge was consumed in the formation of the solid-electrolyte interface (SEI) layer, and hence not retrieved during discharge. During subsequent cycles, the coulombic efficiency was >97%. However, the comparatively low discharge capacity indicates a low cathode utilization, i.e., an incomplete NMC delithiation.

2.4. Reaction Volume of Graphite and NMC

Measuring the OCP in a three-electrode cell while changing the applied pressure (as described in the Experimental Section, see Figures S4 and S5, Supporting Information) enabled calculating the reaction volume of both graphite and NMC separately at various SOCs, as shown in **Figure 3**a. The reaction volume of graphite decreased with SOC, from 7.7 cm^3 mol^{-1} at 0% SOC to 1.2 cm^3 mol^{-1} at 100% SOC. This is mainly due to the increased spacing between the graphene layers as lithium is intercalated.[11,22] The effect is strongest for a low lithium content (low SOC), and decreases as lithium increasingly enters layers that already have a high lithium content. It is worth noting that if the lithiation of graphite would be allowed to continue further, the reaction volume would be expected to increase again as the second intercalation stage is reached.[11,22] This is, however, not observed since the full capacity of the oversized graphite electrode is not utilized. The NMC reaction volume was negligible below 70% SOC, and then increased to 1.8 cm^3 mol^{-1} at 100% SOC. The interplay between several effects in the layered NMC structure determines how it expands and contracts at different SOCs.[9] The details also differ depending on the NMC composition (e.g., Ni content).[8,9] At the beginning of charging, the distance between transition metals (within the layers) decreases with delithiation due to the smaller size of Ni^{4+} compared to Ni^{2+}.[9,23] This is counteracted at the lowest SOCs by an increasing interlayer distance, as the shielding of the negatively charged oxygen atoms is reduced when lithium ions are removed.[9] At high SOCs, the interlayer distance instead shrinks rapidly due to a partial charge transfer to the oxygen atoms, decreasing the interlayer repulsion.[9,23] We note that this particular NMC material exhibits a lower reaction volume at low SOC than is commonly observed,[8,9] even exhibiting close to zero volume change at 20–40% SOC, functioning as a zero-strain material. On the other hand, the positive reaction volume of the NMC cathode at high SOC means that as the cell is charged (NMC delithiated), its volume decreases, alleviating some of the pressure increase from the graphite anode. The observations for both graphite and NMC are in line with previously reported results,[9,11] although the relatively low material utilization seen here leads to a limited range of lithium content for both electrodes. Specifically, only the low lithium content behavior is observed for the graphite anode, while the NMC cathode is limited to a high lithium content. It

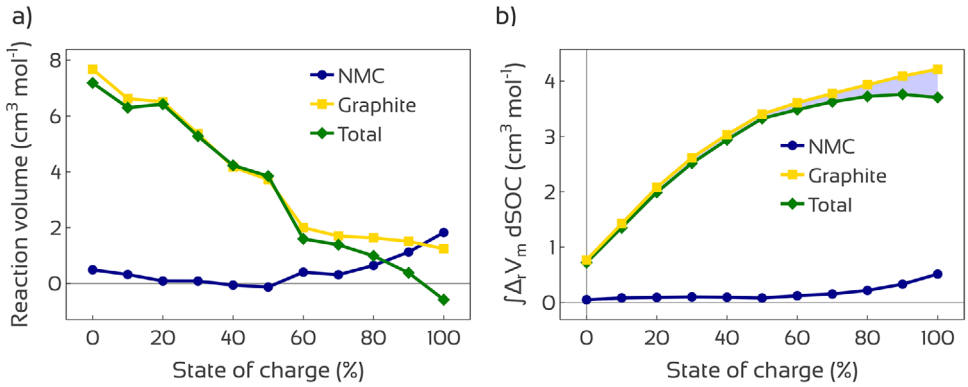

Figure 3. a) Reaction volume and b) the integral of the reaction volume with respect to the state of charge for NMC (blue circles) and graphite (yellow squares), as well as the difference between them (green diamonds), at different states of charge. The shaded blue area corresponds to the NMC contribution to the total.

is also relevant to examine the "total reaction volume", i.e., the difference of the two electrode contributions, which reveals how much the cell expands during the charging process (green curve in Figure 3a). In total, the graphite was responsible for the majority of the reaction volume in this cell, but at 100% SOC, the NMC contraction outweighed the graphite expansion, which should cause the total expansion of the cell to cease, or even slightly contract at the end of the charge step. This can indeed be seen as a flattening of the pressure profile at 100% SOC in **Figure 4**, as described below.

2.5. Disambiguation of Full Cell Breathing

While cycling a two-electrode graphite||NMC cell in a spring-loaded pressure frame, the pressure followed the expansion and contraction of the cell (green curve in Figure 4). The pressure increased by approximately 250 kPa as the cell was charged, followed by a corresponding pressure decrease during discharge.

Having determined the reaction volumes of each electrode as well as the total reaction volume of the cell, we can now calculate how much each electrode contributes to the observed pressure increase during cycling (see Equation (5) in the Experimental Section). Integrating the reaction volume with respect to SOC reveals the cumulative volume change as a result of charging the cell ($\int \Delta_r V_m \, dSOC$, as shown in Figure 3b), which is proportional to the resulting pressure change (Equation (5)). The calculated contribution from the graphite anode to the observed pressure is shown in yellow in Figure 4, while the simultaneous and counteracting effect of NMC is indicated by the blue shaded area. Graphite is clearly the main contributor to the pressure changes observed during cycling, completely overlapping with the total pressure at low and medium SOC. However, at high SOC, the observed pressure increases less than the graphite pressure, since NMC contracts and alleviates some of the graphite breathing.

Relating the reaction volume to the cell breathing in this way is very convenient, since it allows for assigning the pressure variations during cycling to each electrode, without the need for mechanically measuring each one separately, or in situ structure determination methods such as X-ray diffraction. Instead, all that is needed is the inclusion of a zero-strain reference electrode in the solid-state cell, as well as precise control and measurement of the pressure applied to the cell stack. Absolute accuracy of the

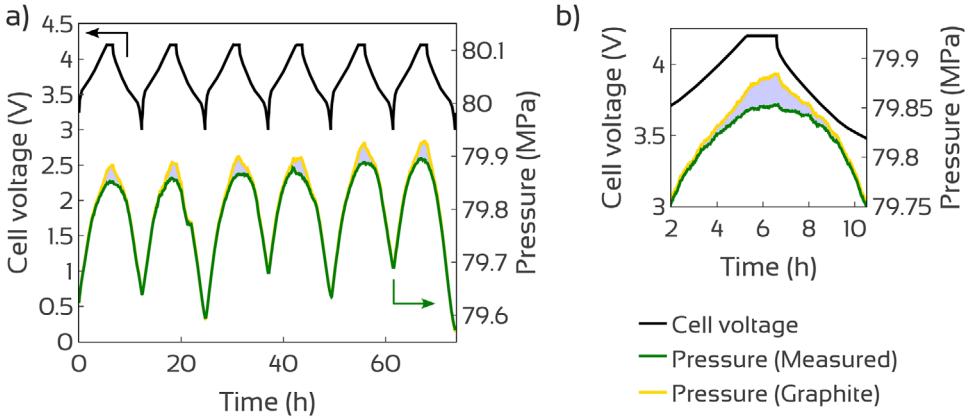

Figure 4. a) Cycling excerpt for a two-electrode graphite|LPSCl|NMC cell. Cell voltage (black, left y-axis), the total measured pressure (green, right y-axis), and the calculated pressure contribution from the graphite anode (yellow, right y-axis). The shaded blue area corresponds to the pressure reduction contribution from the NMC cathode. b) Close-up of a portion of the first cycle.

recorded pressure values is, however, not necessary, since only the change in pressure is relevant, rather than the absolute applied pressure (see Equation (2) in the Experimental Section). If the pressure change cannot be accurately measured (e.g., due to a drifting pressure or excessive noise in the force signal), the calculated reaction volume will have a proportional error as well. The same considerations hold for the OCP determination by a potentiostat, i.e., a bias potential has no effect on the determined reaction volume values, but OCP differences of a few millivolts or less must be possible to measure accurately. Moreover, the ability to automate the application of different pressure programs (like in Figure S1, Supporting Information), as well as integration with electrochemical methods (like the battery cell cycling performed here), greatly simplifies the procedure.

Measuring the pressure for cycling cells in operando can yield important information for improving cell performance and cycle life. Reducing the overall pressure swings is generally desirable both for improving the cell performance and to allow for mechanically simpler battery modules.[24] The applied pressure will also affect the ionic conductivity of the solid electrolyte,[25] and for lithium metal electrodes, the pressure also has a large impact on the lithium plating quality.[21] Determining the breathing behavior of each electrode provides more specific information that can aid in further improving cell performance. Matching the breathing of the anode and cathode so that their effects cancel out could greatly reduce the total cell pressure swings.[8] However, not only the total cell breathing, but also the individual electrode breathing, is important. The electrode volume changes are related to particle cracking and capacity fading for many active materials, and this problem will persist even if the other electrode negates the expansion.[4,5,6] One way to tackle this problem is to adjust the stiffness of the electrode materials as well as the solid electrolyte. Softer materials such as sulfidic electrolytes can absorb the volume changes and reduce the overall pressure swings.[1,26] While the electrode porosity in liquid-electrolyte battery cells can accommodate some of the breathing, this is not possible in densely compacted solid-electrolyte battery cells.[24] Furthermore, while liquid electrolytes can enter newly formed cracks in the active material particles to achieve a level of "self-healing", solid electrolytes do not have this ability.[4] As a result, the electrode material breathing leads to much more severe consequences with solid electrolytes, and it is crucial to understand this phenomenon in order to design a well-performing (large-format) all-solid-state battery.

3. Conclusion

The simultaneous in situ determination of the reaction volumes of both anode and cathode in solid-state battery cells has been demonstrated by using an LTO-based reference electrode. The reaction volumes of graphite and NMC at different degrees of lithiation were measured in this way, as were the reaction volumes of Li and InLi at different temperatures. The cell breathing during cycling of a graphite|LPSCl|NMC cell could thus be disambiguated into the separate anode and cathode contributions. In this cell, the graphite anode expansion was responsible for the majority of the pressure increase during charging, while the contraction of the NMC cathode at high SOCs counteracted that pressure increase, leading to an observed pressure plateau at the end of charge.

The LTO reference electrode was very stable with a drift of less than 0.2 mV per day for several months, since the reference potential (1.565 V vs Li at zero pressure and 25 °C) is much less reductive than other commonly employed reference electrode materials such as Li or InLi. This improves the electrochemical compatibility with common solid electrolytes and enables long-term three-electrode experiments, allowing for the differentiation of the anode and cathode contributions to the cell voltage. The LTO reference potential is also invariable with pressure, which is necessary for the accurate determination of reaction volumes using this method. By relating the reaction volume to the cell breathing, information about the individual electrode volume changes can be obtained without the need for additional characterization techniques. Quantifying the volume changes of the solid-state battery active materials is critical for improving their performance, especially when transitioning to large-format cells.

4. Experimental Section

Fabrication of LTO Coated Reference Wire Electrodes: Pristine $Li_4Ti_5O_{12}$ powder was partially lithiated to form an equimolar mixture of $Li_4Ti_5O_{12}$ and $Li_7Ti_5O_{12}$, in accordance with a procedure by Ikezawa et al.:[13] First, a naphthalene solution was prepared by adding naphthalene (6.5 mmol, ≥99.6%, Thermo Fisher Scientific) in anhydrous tetrahydrofuran (THF, 30 cm^3, Merck) and stirring for 2 h. Lithium metal (6.5 mmol, Honjo Japan) was added to this solution and stirred for 24 h to form a dark green solution of lithium naphthalenide. $Li_4Ti_5O_{12}$ powder (2 g, NEI corporation) was added to this and stirred for 6 h at 250 rpm. The $Li_4Ti_5O_{12}$/$Li_7Ti_5O_{12}$ suspension was later filtered, and the recovered dark blue powder was dried under vacuum for 24 h at 80 °C. All reactions were carried out at room temperature (around 25 °C) in an argon-filled glovebox (≤0.1 ppm H_2O and ≤0.1 ppm O_2). A glass-coated magnetic stirrer and a 50 mL borosilicate glass container with a lid were used for carrying out the reaction. A detailed description of the synthesis procedure and material characterization will be published elsewhere.[27]

LTO-coated wires were produced by slurry coating, using polyisobutene (Oppanol B 150, BASF) dissolved in THF (2.5% m/m) as binder. The slurry was prepared by mixing reduced LTO (95 mg) with the binder solution (200 mg) using a mortar and pestle in an argon-filled glovebox. Additional THF was also added to adjust the slurry viscosity during the wire coating process, since THF is prone to rapid evaporation. Ni wires (100 µm Ø) were stretched out, put under tension, and dipped horizontally into the slurry, which was spread on a flat surface, to coat the wire surface. The coated wires were left in the glovebox for 30 min to allow the solvent to evaporate, before being dried in a vacuum oven at 60 °C for 24 h. The wires were kept under argon until being used as reference electrodes.

Two- and Three-Electrode Cell Assembly: Cell stacks were assembled in a CompreCell 12DP (rhd instruments GmbH & Co. KG) measurement cell with 12 mm sample diameter.[15] Studies of solid-state battery electrode breathing using this measurement cell have recently been reported by others, both with passive and active pressure control.[7,28] The cell features exchangeable sleeves for use in either two- or three-electrode mode. The anode and cathode were contacted by two tungsten carbide hard-metal pistons that also communicate the pressure to the cell stack. All cell parts were dried in a vacuum oven at 60 °C for 12 h before being transferred into an argon-filled glovebox for assembling the cell stack. Cell assembly and pre-compression of the electrolyte and electrode layers were performed at room temperature (around 22 °C).

Li_6PS_5Cl (LPSCl, 325 mesh, Ampcera) was used as electrolyte for all tests. $LiNi_{0.6}Mn_{0.2}Co_{0.2}O_2$ (65%, NMC622, BASF) was mixed with LPSCl (32%) and carbon black (3%, C65, Imerys Graphite & Carbon) to form the

cathode composite. Natural graphite (68%, 918-II, MTR) was mixed with LPSCl (32%) to form the anode composite.

Graphite|LPSCl|NMC two-electrode cells were prepared by first pressing LPSCl (100 mg cm^{-2}) into a polyetherimide (PEI) sleeve by applying 100 MPa for 5 min in a ComPrep pressure application frame (rhd instruments GmbH & Co. KG). NMC composite (20.7 mg cm^{-2}) and graphite composite (21.0 mg cm^{-2}) were then added to either side of the LPSCl pellet. The cell was pressed with 500 MPa for 5 min in a CompreDrive (rhd instruments GmbH & Co. KG) to complete the compaction and ensure good interfacial contact between all layers in the cell.

Graphite|LPSCl|NMC three-electrode cells were assembled in a polyether ether ketone (PEEK) sleeve equipped with an LTO-coated Ni wire reference electrode. After assembly, the reference electrode wire goes through the center of the electrolyte, along the diameter. This was accomplished by pressing equal amounts of LPSCl onto each side of the reference electrode (in total 200 mg cm^{-2}), applying 150 MPa for 5 min in a ComPrep. The anode and cathode were added as described above, followed by compression with 300 MPa for 5 min in a CompreDrive. This lower pressure was chosen to avoid mechanical shearing of the LTO coating.

For Li|LPSCl|LiIn three-electrode cells, the electrolyte layer with an LTO reference electrode wire was prepared as described above. Li foil (50 µm, 11.9 mm Ø, Honjo Japan) and In foil (100 µm, 11.9 mm Ø, Goodfellow) were added to one side of the LPSCl pellet (Li towards the electrolyte), and Li foil to the other. A CompreDrive was used to apply 50 MPa to the cell for 45 min to ensure the formation of the InLi alloy, as well as good electrolyte interfacial contact. The LiIn formation could be confirmed by the change in OCP from -1.56 to -0.95 V versus LTO (i.e., from 0.00 to 0.62 V vs Li).

Mechanical and Electrochemical Characterization: Charge/discharge cycling of the two-electrode graphite||NMC cell was performed in a CompreFrame (rhd instruments GmbH & Co. KG) adjusted to apply a pressure of 80 MPa. All other experiments were conducted in a CompreDrive. The CompreFrame is a spring-loaded pressure application frame ("pseudo-constant pressure control"[29]), i.e., any cell expansion or contraction will result in a measurable pressure change. The CompreDrive, on the other hand, is an actively regulated pressure application setup that continuously regulates the cell compression to keep the pressure completely constant, even when the cell experiences volume changes ("true constant pressure control"[29]). This is accomplished with proportional-integral-derivative (PID) control of a servo motor in a closed feedback loop with a force sensor. In all cases, an HC-addon (rhd instruments GmbH & Co. KG) was used to regulate the temperature, and all tests of the graphite||NMC cells were performed at 25 °C. Using the CompreDriveControl 1.16 control software (rhd instruments GmbH & Co. KG), the pressure and temperature procedures necessary for the measurements in this study could be completely automated.

An SP-200 and an SP-240 potentiostat (Biologic) were used for all electrochemical measurements. Constant current (CC) charging was done at C/10 (using a nominal capacity of 200 mAh g^{-1} for NMC, which is the limiting electrode) until a cell voltage of 4.2 V, followed by a constant cell voltage (CV) step until C/50. Next, CC discharge was performed at C/10 until 3.0 V, followed by a 10-min rest period. The differential capacity (dQ/dE) was calculated by interpolating the capacity in a 1-mV evenly spaced potential range, differentiating with respect to the potential, and then applying Whittaker–Henderson smoothing (2nd order, $\lambda = 1000$). dQ/dE was defined as negative for the charge step and positive for the discharge step.

Reaction Volume Determination: The reaction volumes of Li and InLi were measured by applying a combined temperature/pressure ramp procedure (Figure S1, Supporting Information) in which the OCP for each electrode was recorded continuously while 5 MPa – 50 MPa was applied in 5 MPa increments for 5 min each. The reverse sweep (50 MPa – 5 MPa) was then also applied, in order to cancel out any effects of a small drift in OCP. This was repeated at different temperatures in the range from 10 to 60 °C.

The reaction volumes of graphite and NMC were measured in the three-electrode graphite||NMC cell, which first underwent one formation cycle at 200 MPa as described above. The OCP for each electrode was then recorded during a pressure procedure of 200 MPa – 20 MPa – 200 MPa (5 minutes for each step) in the discharged state. The cell was then charged by CC/CV as described above with the pressure procedure repeated every 10% SOC, based on the actual discharge capacity (144 mAh g_{NMC}^{-1}), with a 4-hour rest period at each point.

The molar reaction volume can be expressed as the change in volume (V) during a reaction, such as the insertion of lithium into a structure:

$$\Delta_r V_m = \frac{dV}{dn_{Li}} \tag{1}$$

where n_{Li} is the amount of lithium inserted into the structure.[8] The reaction volume can also be calculated based on the change in OCP (E_{OC}) when changing the applied pressure (p) while keeping the temperature and SOC constant. For the insertion of one lithium ion:

$$\Delta_r V_m = -F\frac{dE_{OC}}{dp} \tag{2}$$

where F is the Faraday constant.[8] The derivative of OCP with respect to pressure was determined by linear fitting of the OCP values measured at the end of each pressure step described above. Assuming a constant reaction volume in a certain pressure range, the reduction potential at some pressure ($E(p)$) can be calculated knowing the reduction potential at zero pressure and the reaction volume:

$$E\ (p) = E_{p=0} - p \cdot \frac{\Delta_r V_m}{F} \tag{3}$$

The total volume change (ΔV) during the charging process of a battery electrode is the integral of the reaction volume with respect to n_{Li}:

$$\Delta V = \int \Delta_r V_m dn_{Li} \tag{4}$$

Since the volume expansion is constrained to the direction of the applied pressure in these cells (i.e., the cross-section area is constant), the height change (Δh) is proportional to ΔV. When operated in a spring-loaded pressure application frame such as the CompreFrame, the pressure change (Δp) is proportional to Δh through the spring constant.[29] Furthermore, the SOC is proportional to the amount of lithium ions inserted into the anode and extracted from the cathode. Hence:

$$\Delta p \propto \int \Delta_r V_m dSOC \tag{5}$$

In this way, the reaction volume was calculated for both anode and cathode in the three-electrode cells. The total reaction volume for the cell charging process (i.e., the net volume increase during the charging process) was calculated as the difference between the anode and cathode reaction volumes (the cathode contribution is negated since it is delithiated during the charging process). The total contribution to the pressure change from each electrode could then be calculated at each SOC, since it is proportional to the reaction volume contribution.

Statistical Analysis: No statistical hypothesis testing was applied in this study. No data normalization or outlier exclusion was performed. Edelweiss 0.1 (rhd instruments GmbH & Co. KG) was used to synchronize the potentiostat and pressure data sets, as well as for all other data analysis and figures herein.

Supporting Information

Supporting Information is available from the Wiley Online Library or from the author.

Acknowledgements

This study was performed within the project REFA (Grant Nos. 03EI6055A + 03EI6055B), funded by the German Federal Ministry of Economic Affairs and Energy (BMWE) as part of the 7. Energieforschungsprogramm, which is highly appreciated.

Conflict of Interest

The authors declare no conflict of interest.

Data Availability Statement

The data that support the findings of this study are available from the corresponding author upon reasonable request.

Keywords

cell breathing, lithium-ion batteries, reaction volume, solid-state batteries, three-electrode setup

Received: August 1, 2025
Revised: August 21, 2025
Published online:

[1] S. Kalnaus, N. J. Dudney, A. S. Westover, E. Herbert, S. Hackney, *Science* **2023**, *381*, abg5998.
[2] A. Joshi, D. K. Mishra, R. Singh, J. Zhang, Y. Ding, *Appl. Energy* **2025**, *386*, 125546.
[3] P. Daubinger, M. Göttlinger, S. Hartmann, G. A. Giffin, *Batteries Supercaps* **2023**, *6*, 202200452.
[4] R. Ruess, S. Schweidler, H. Hemmelmann, G. Conforto, A. Bielefeld, D. A. Weber, J. Sann, M. T. Elm, J. Janek, *J. Electrochem. Soc.* **2020**, *167*, 100532.
[5] T. Shi, Y.-Q. Zhang, Q. Tu, Y. Wang, M. C. Scott, G. Ceder, *J. Mater. Chem. A* **2020**, *8*, 17399.
[6] H. Huo, Y. Bai, S. L. Benz, T. Weintraut, S. Wang, A. Henss, D. Raabe, J. Janek, *Adv. Mater.* **2025**, *37*, 2415006.
[7] E. Sánchez-Ahijón, A. Pendashteh, J. J. Vilatela, *Batteries Supercaps* **2024**, *7*, 202400292.
[8] R. Koerver, W. Zhang, L. D. Biasi, S. Schweidler, A. O. Kondrakov, S. Kolling, T. Brezesinski, P. Hartmann, W. G. Zeier, J. Janek, *Energy Environ. Sci.* **2018**, *11*, 2142.
[9] L. D. Biasi, A. O. Kondrakov, H. Geßwein, T. Brezesinski, P. Hartmann, J. Janek, *J. Phys. Chem. C* **2017**, *121*, 26163.
[10] W. Zhang, D. Schröder, T. Arlt, I. Manke, R. Koerver, R. Pinedo, D. A. Weber, J. Sann, W. G. Zeier, J. Janek, *J. Mater. Chem. A* **2017**, *5*, 9929.
[11] S. Schweidler, L. D. Biasi, A. Schiele, P. Hartmann, T. Brezesinski, J. Janek, *J. Phys. Chem. C* **2018**, *122*, 8829.
[12] T. Ohzuku, A. Ueda, N. Yamamoto, *J. Electrochem. Soc.* **1995**, *142*, 1431.
[13] A. Ikezawa, G. Fukunishi, T. Okajima, F. Kitamura, K. Suzuki, M. Hirayama, R. Kanno, H. Arai, *Electrochem. Commun.* **2020**, *116*, 106743.
[14] K. Yoshida, A. Ikezawa, T. Okajima, H. Arai, *Electrochim. Acta* **2024**, *497*, 144523.
[15] C. Karlsson, "Application Note: Three-Electrode All-Solid-State Battery Cycling," rhd instruments magazine, https://rhd-instruments.de/magazine/three-electrode-all-solid-state-battery-cycling/ (accessed: December 2023).
[16] J. Hertle, F. Walther, B. Mogwitz, S. Schröder, X. Wu, F. H. Richter, J. Janek, *J. Electrochem. Soc.* **2023**, *170*, 040519.
[17] G. F. Dewald, S. Ohno, M. A. Kraft, R. Koerver, P. Till, N. M. Vargas-Barbosa, J. Janek, W. G. Zeier, *Chem. Mater.* **2019**, *31*, 8328.
[18] B. Hallstedt, *Calphad* **2007**, *31*, 292.
[19] P. Hidnert, M. G. Blair, *J. Res. Natl. Bur. Stand.* **1943**, *30*, 427.
[20] W. A. Alexander, L. D. Calvert, R. H. Gamble, K. Schinzel, *Can. J. Chem.* **1976**, *54*, 1052.
[21] K. B. Hatzell, X. C. Chen, C. L. Cobb, N. P. Dasgupta, M. B. Dixit, L. E. Marbella, M. T. McDowell, P. P. Mukherjee, A. Verma, V. Viswanathan, A. S. Westover, W. G. Zeier, *ACS Energy Lett.* **2020**, *5*, 922.
[22] J. K. Mathiesen, R. E. Johnsen, A. S. Blennow, P. Norby, *Carbon* **2019**, *153*, 347.
[23] A. O. Kondrakov, H. Geßwein, K. Galdina, L. de Biasi, V. Meded, E. O. Filatova, G. Schumacher, W. Wenzel, P. Hartmann, T. Brezesinski, J. Janek, *J. Phys. Chem. C* **2017**, *121*, 24381.
[24] H. Pegel, O. V. Kessel, P. Heugel, T. Deich, J. Tübke, K. P. Birke, D. U. Sauer, *J. Power Sources* **2022**, *537*, 231443.
[25] C. Schneider, C. P. Schmidt, A. Neumann, M. Clausnitzer, M. Sadowski, S. Harm, C. Meier, T. Danner, K. Albe, A. Latz, W. A. Wall, B. V. Lotsch, *Advanced Energy Materials* **2023**, *13*, 2203873.
[26] J. H. Teo, F. Strauss, F. Walther, Y. Ma, S. Payandeh, T. Scherer, M. Bianchini, J. Janek, T. Brezesinski, *Mater. Futures* **2022**, *1*, 015102.
[27] M. Soans, D. Bresser, A. Varzi, "THF-Based Binder System for Stable Slurry Preparation of Partially Lithiated Li4Ti5O12 for Enabling Wire-Type Reference Electrode Preparation for Solid-State Battery Applications," In preparation, **2025**.
[28] C. D. Alt, S. Keuntje, I. L. Schneider, J. Westphal, P. Minnmann, J. K. Eckhardt, K. Peppler, J. Janek, *Adv. Energy Mater.* **2025**, *15*, 2404055.
[29] C. Karlsson, "Application note: Introducing: True Constant Volume Pouch Cell Cycling," rhd instruments magazine, https://rhd-instruments.de/magazine/introducing-true-constant-volume-pouch-cell-cycling/ (accessed: January 2025).